Hyper Triplet-Triplet Fusion Blue Fluorescent Organic Light-Emitting Diode

Chia-Hsun Chen
Pei-Hsi Lee
National Taiwan University
Hung-Yi Lin
National Taiwan University
Bo-Yen Lin
Yuan Ze University
Man-kit Leung
National Taiwan University
Tien-Lung Chiu (tlchiu@saturn.yzu.edu.tw)
Yuan Ze University https://orcid.org/0000-0002-0631-660X
Jiun-Haw Lee
National Taiwan University

Article

Keywords: blue organic light-emitting diode (OLED), triplet-triplet fusion (TTF), triplet-polaron quenching (TPQ), hyper-TTF, triplet tank layer (TTL), singlet, triplet

Posted Date: March 10th, 2022

DOI: https://doi.org/10.21203/rs.3.rs-994123/v1

Abstract

Triplet is like a double-edged knife, that can degrade or benefit the electroluminescence performances of organic light-emitting diodes (OLEDs), especially for blue light. Therefore, efficient triplet harvesting for triplet-triplet fusion (TTF) fluorescence emission is essential to achieving high-efficiency blue TTF-OLEDs, which are known for their excellent reliability. This study presents a hyper-TTF mechanism for maximizing triplet exciton usage and avoiding triplet-polaron quenching to generate more photons through Dexter energy transfer (DET) and TTF processes. Specially, a triplet tank layer (TTL) was introduced adjacent to the TTF emitting layer (EML). Efficient carrier recombination and triplet generation are confined to the TTL of the device. Most triplets were observed to undergo DET from the TTL to the TTF EML; they subsequently became singlets exhibiting delayed fluorescence. Furthermore, the triplet-polaron quenching is suppressed by inhibiting hole into the TTF EML. A record-high TTF-OLED efficiency was achieved with an external quantum efficiency of 15.4%.

Full Text

According to spin statistics of organic light-emitting diodes (OLEDs), 25% singlet excitons and 75% triplet excitons are generated by electrical excitation. Efficient utilization of triplet excitons in light emission is essential for achieving high-efficiency OLEDs. Triplet excitons are implicated in three common emission mechanisms: phosphorescence (Ph), thermally activated delayed fluorescence (TADF), and triplet-triplet fusion (TTF) fluorescence. Improving intersystem crossing (ISC) and reducing the radiative lifetime of triplet excitons can enable Ph-OLED to exhibit a theoretical internal quantum efficiency (IQE) value (η_{IQE}) of 100%. Ph-OLED have had great success in red and green emitters in mass-produced OLED displays[1,2]. For TADF emitters, the triplet state is raised close to the singlet state to facilitate reverse intersystem crossing (RISC).[3] Nonemissive triplet excitons go RISC to singlet state because of thermal energy and then produce singlet emission (fluorescence), thus manifesting a theoretical η_{IQE} of 100%[4,5]. Nevertheless, stability of high-efficiency blue Ph- and TADF-OLEDs is still an issue primarily engendered by the high-energy and long-life triplet excitons, whose triplet-polaron annihilation process generate hot polarons that aggravate the material degradation[6]. To avoid hot polaron formation to achieve improved stability of blue OLEDs, the use of low-triplet-state anthracene- or pyrene-based compounds is a reliable approach in display products with TTF emission mechanism, especially for deep-blue emitters[7]. However, concerns about the efficiency of TTF-OLED remain because the exciton amount decreases when two triplet excitons are converted into one singlet exciton. The η_{IQE} upper limit of TTF is 62.5% (25% + 75%/2). Furthermore, the ideal external quantum efficiency (EQE) value (η_{EQE}) can be calculated as 12.5–25%—depending on the light extraction efficiency (η_{LE}) of 20–40%—using the following theorems[8]:

$$\eta_{EQE} = \eta_{IQE} \times \eta_{LE} \quad (1)$$

$$\eta_{IQE} = \eta_{Re} \times \chi \times \eta_{PLQY} \quad (2)$$

Where η_{Re} is recombination efficiency, χ is radiative exciton ratio, and η_{PLQY} is photoluminescence quantum efficiency (PLQY) value. In the past five decades, the highest reported η_{EQE} of anthracene- or pyrene-based blue TTF-OLEDs was no more than 12%[9], which is less than the minimal theoretical value of 12.5% (with η_{LE} = 20%). Although numerous strategies have been employed to improve the efficiency of blue TTF-OLEDs, including material development and device design, devices still have difficulty reaching the minimum theoretical efficiency[10]. Several factors are responsible for this, with the major one being that triplet–polaron quenching (TPQ) decreases the amount of triplet excitons, resulting in an inefficient TTF process[9]. Injecting more carriers into an emitting layer (EML) to increase excitons formation is an appealing approach[7]. However, in a conventional TTF-OLED single-EML structure, balancing exciton and carrier numbers is a problem because carriers generate and quench excitons concurrently. Generating more excitons requires more carriers, but more carriers result in increased TPQ because excitons and carriers stay close together. To avoid TPQ, we propose a novel hyper–TTF EML structure that efficiently utilises triplet excitons by introducing a carrier recombination layer to efficiently emit the singlet excitons and transfer triplet excitons to the other layer for TTF emission.

Results

Structurally, a traditional TTF-OLED comprises a single EML for carrier recombination, exciton generation, TTF process, and singlet photon emission, as depicted in Fig. 1a. Therefore, TPQ is unavoidable to decrease the amount of triplet excitons because triplet excitons and polarons are free in the same space, which also suppresses the TTF process and singlet exciton formation. To reduce TPQ, we modified the conventional single EML of a TTF-OLED by adding a triplet tank layer (TTL) adjacent to the TTF EML in order to efficiently generate triplet excitons and transfer them to the TTF EML to trigger a delocalised TTF process, also called a hyper–TTF process. The primary condition for TTL establishment in a device is a triplet-exciton-rich region, that is, the main carrier recombination zone and the major prompt fluorescence (PF) EML of the device. In a hyper–TTF-OLED structure, the main carrier recombination zone is spatially separated from the TTF zone. Definitely, the device can be engineered to ensure that the main carrier recombination zone is located on the TTL. The required material properties for a TTL are high η_{PLQY}, efficient Dexter energy transfer, and no TTF behavior. In this study, a pyrene-based material, 1-(2,5-dimethyl-4-(1-pyrenyl)phenyl)pyrene (DMPPP), was used as the of TTL material and a 9,10-bis(2'-naphthyl)anthracene (ADN) was used as the traditional TTF EML. The singlet/triplet energies and molecular structures are presented in Fig. 1b. DMPPP was determined to have a high η_{PLQY} value (63.5%; **Supplementary Fig. S1**) and to insufficiently trigger TTF. Moreover, its triplet excitons diffused to the adjacent ADN layer for TTF and singlet exciton generation. The structures of the traditional TTF- and hyper–TTF-OLEDs were ITO/TAPC (40 nm)/NPB (10 nm)/ADN (10 nm)/BPhen (55 nm)/LiF (1 nm)/Al (100 nm) and ITO/TAPC (40 nm)/NPB (10 nm)/DMPPP (5 nm)/ADN (10 nm)/BPhen (55 nm)/LiF (1 nm)/Al (100 nm), respectively; here, ITO represents indium tin oxide serving as anode, NPB represents *N*-diphenyl-*N*,*N*-bis(1-napthyl)-1,1'-biphenyl-4,4'-diamine serving as hole transporting layer, BPhen represents bathophenanthroline serving as electron transporting layer (ETL), LiF represents lithium fluoride serving

as electron injection layer, and Al represents aluminum serving as cathode. The turn-off dynamics, time-resolved electroluminescence (TREL) analysis results (obtained after operated at their maximum η_{EQE} with a current density of approximately 4 mA·cm^{-2}), and η_{EQE} versus current density plots for TTF- and hyper–TTF-OLEDs are displayed in Figs. 1c and 1d, respectively. According to the TREL signal profiles on a time scale of 15 μs, two-slop patterns with a prompt and a delayed signal were identified and could be attributed to PF and delayed fluorescence (DF), respectively; this resulted from the singlet excitons produced individually through direct carrier recombination and indirect TTF. The inflection point of the two-slop TREL curve represents the DF emission ratio, corresponding to the proportion of triplet excitons that contributed to TTF emission. The theoretical value of the DF emission ratio was determined to be 60%. In the reference TTF-OLED, the derived DF emission constituted 7% of total intensity, which is consistent with typical reported values[7]. Notably, the DF emission ratio observed for the hyper–TTF-OLED was 47% of total intensity, which was attributed to reduced TPQ. The triplet excitons in TTL was depleted and underwent TTF by ADN layer, contributing to the delayed emission. As the current density varied, the TPQ effect fluctuated, which affected the delayed emission ratio. Therefore, the contributions of PF and DF to the device EQEs could be calculated separately as bar graph in Fig. 1d; the PF and DF emission characteristics of the devices at the maximum η_{EQE} are summarised in **Table 1**. The hyper–TTF-OLED exhibited deep-blue emission with CIE1931 colour coordinates of (0.15, 0.07), similar to those for the reference TTF-OLED. In particular, at the maximum η_{EQE}, the η_{EQE} value of the hyper–TTF-OLED was 4.12%, much greater than that of reference TTF-OLED (1.97%). The η_{EQE} enhancement was attributed to the increases in PF and DF emission. The obvious increment in the DF η_{EQE} value from 0.14–1.9% was crucial because the TTL enabled the separation of the carrier recombination zone and the TTF zone to reduce the TPQ effect. The small increase in PF η_{EQE} was due to the high η_{PLQY} DMPPP. The proportion of η_{EQE} contributed by DF increased with raising current density (range: 1–100 mA·cm^{-2}), which was easily observed in the reference TTF-OLED (from 6–10%). This is because the probability of TTF increased when the density of triplet excitons in the EML was high at a high current density. Particularly, in the hyper–TTF-OLED, as the current density increased, only a little increase (from 47–48%) in η_{EQE} contributed by DF could be detected, demonstrating the usage of triplet excitons is efficient, including faster DET from the DMPPP to the ADN and less TPQ in the DMPPP and ADN layers. Notably, DMPPP is insensitive to TPQ, unlike ADN. To realise the TPQ effect in ADN, we explored whether its TTF process could be quenched by positive or negative polarons. Two optical pumping TTF hole- and electron-only devices (HOD and EOD, respectively) were fabricated. The structures of the fabricated HOD and EOD were ITO/MoO_3 (10 nm)/ADN (40 nm)/ADN: 40% Platinum octaethylporphyrin (PtOEP; 10 nm)/ADN (40 nm)/MoO_3 (10 nm)/Al and ITO/1,3,5-tri(m-pyridin-3-ylphenyl)benzene (TmPyPb; 10 nm)/ADN (40 nm)/ADN: 40% PtOEP (10 nm)/ADN (40 nm)/TmPyPb (10 nm)/LiF/Al, respectively. PtOEP is a red phosphorescent emitter that was applied in this study to absorb optical excitation (a 532-nm picosecond laser) to generate triplet excitons[3] and then DET to ADN for TTF; this is illustrated by the exciton kinetics in **Supplementary Fig. S2**. When the devices were driven under various current densities and simultaneously pumped by optical excitation, the intensity of the DF blue emission through TTF (I_{TTF}) was monitored, as displayed in Fig. 1e. The photoluminescence (PL) spectra and time-resolved PL (TRPL)

signals of the DF blue emission for the EOD and HOD are displayed in **Supplementary Figs. S3a–S3d**. As current density increased, I_{TTF} decreased, indicating that the polarons reduced the amount of triplet excitons and dampened the TTF process, demonstrating the TPQ effect. I_{TTF} decreased the most in the HOD, indicating that triplet excitons are responsive to positive polarons (h^+) but less so to negative polarons (e^-). Notably, the TPQ effect was imperceptible on PtOEP because the PL Ph emission spectra in the range 600–650 nm from the PtOEP in the EOD and HOD under various current densities exhibited an identical spectrum (**Supplementary Figs. S3e** and **S3f**). Therefore, one can conclude that TPQ relies only on the triplet exciton of ADN, especially for h^+-induced TPQ. In particular, the TPQ effect was aggravated in the single-carrier devices (EOD and HOD) because the devices rapidly accumulated excessive polarons without carrier recombination mechanism, which facilitated the quenching of the triplet excitons. In efficient OLEDs, few polarons can accumulate because most carriers efficiently recombine to form excitons. Major polarons come from the transporting carriers on the way to recombination. Because h^+-induced TPQ on the ADN is disastrous, the intention to reduce the h^+-induced TPQ and increase the usage of triplet excitons is inhibiting the entry of h^+ into the ADN layer, as a schematic of carrier and exciton dynamics in the hyper–TTF-OLED presented in Fig. 1b. Therefore, the high efficiency of the hyper–TTF-OLED can be attributed to the increased DF contribution.

To ensure that the main carrier recombination zone was located on the TTL, an Alq_3 dopant (5%, 1 nm) as the probe was employed to explore singlets at three EML positions in three hyper–TTF-OLEDs (Fig. 2a). When the DMPPP/ADN interface position was set to zero, the Alq_3 probe was doped at three positions, namely −4.5, 0.5, and 9.5 nm, in the devices. The blue singlet excitons of DMPPP and ADN were transformed into green singlet excitons of the Alq_3 probe through Förster resonance energy transfer (FRET) (**Supplementary Fig. S4**). On the contrary, triplet excitons didn't transfer to the Alq_3 probe due to the relatively high triplet energy of Alq_3. The detail EL performances of the devices are detailed in **Supplementary Fig. S5**. The maximum η_{EQE} of these three devices and the contributions of PF and DF to the blue and green η_{EQE} results are summarised in **Table 2**. Individual blue and green emissions were identified through spectral splitting (Fig. 2b), and the corresponding PF and DF ratios were determined through TREL measurement with a spectral filter. The greatest green PF η_{EQE} from the Alq_3 probe at the position of −4.5 nm, indicating that the main recombination zone was located on the TTL; where the blue PF η_{EQE} was small because of the strong FRET from blue to green. The FRET ability decreased with increasing distance away from the main recombination zone, leading to decreased green PF η_{EQE} at the 10-nm case. In contrast to the green PF η_{EQE}, the η_{EQE} value under green DF approached zero at −4.5 nm and then increased to a peak at 1 nm, signifying that no TTF occurred in the DMPPP TTL and that maximum TTF occurred in the ADN region near the DMPPP/ADN interface. The region located near 1 nm was a triplet-exciton-rich region that benefitted TTF. The triplet excitons in ADN originated from the DMPPP TTL through DET. Accordingly, this also exactly proves the concept of exciton dynamics in the hyper TTF-OLED (Fig. 1b).

Nevertheless, the maximum η_{EQE} of 5.41% of the hyper TTF-OLED was low because of the low η_{PLQY} values of the intrinsic DMPPP (63.5%) and ADN (37%) layers (**Supplementary Figs. S1a and S6a**). To improve device efficiency, a high-PLQY dopant was employed to raise the η_{PLQY} of the EML out of necessity. After the DMPPP and ADN thin film were doped with 5% and 3% 7,7,13,13-tetramethyl-N5,N5,N11,N11-tetraphenyl-7,13-dihydrobenzo-[g]indeno[1,2-b]fluorene-5,11-diamine (DPaNIF), the η_{PLQY} values of the DMPPP and ADN mixtures increased to 99% and 96%, respectively (**Supplementary Figs. S1c and S6c**). Employing the mixtures to be the TTL and TTF-EML of the hyper–TTF-OLED, as named 'Hyper-1', the maximum device η_{EQE} value raised to 8.8% (Fig. 3a and **Table 3**; for detail EL characteristics, see **Supplementary Fig. S7**), composing of PF η_{EQE} (5.9%) and DF η_{EQE} (2.9%). The increased colour coordinate CIEy was relied on the DPaNIF emission. However, the DF ratio decreased to 33% (Fig. 3b) because the favorable host packing was disrupted by the incorporated dopant or because partial triplet excitons were inevitably quenched by the DPaNIF dopants with a low triplet energy (E_T = 2.0 eV, see **Supplementary Fig. S8**)[,]. To further promote device efficiency, 9-(1-naphthalenyl)-10-(4-(2-naphthalenyl)phenyl)anthracene (NPAN) was introduced to replace the ADN host in TTF EML because the NAPAN:3%DPaNIF thin film had a relatively high η_{PLQY} value of 97% (**Supplementary Fig. S9**). In addition, to facilitate carrier transport behavior and generate more excitons in the hyper–TTF-OLED, tris(4-carbazoyl-9-ylphenyl)amine (TCTA) and 1,3,5-tri(m-pyridin-3-ylphenyl)benzene (TmPyPb) with high hole and electron mobility were used to replace NPB and Bphen, respectively. The developed high-efficiency hyper–TTF-OLED structure was composed of ITO/ TAPC (40 nm)/ TCTA (10 nm)/ DMPPP:5%DPaNIF (5 nm)/ NPAN:3%DPaNIF (10 nm) / TmPyPb (55 nm)/ LiF (1 nm)/ Al (100 nm), as named 'Hyper-2', which exhibited a maximum η_{EQE} value of 15.4% at luminance of 808 cd·m^{-2} (Fig. 3a and **Table 3**; for detail EL characteristics, see **Supplementary Fig. S7**). This value is a record-high η_{EQE} for a blue TTF-OLED, especially for anthracene- and pyrene-based TTF-OLEDs (Fig. 3c and **Supplementary Table S1**). To this record-high η_{EQE}, PF contributed 10.3% and DF contributed 5.1%. The DF ratio was maintained at 33% (Fig. 3b) because the same parameter settings were used for the DPANIF emitter. To this record-high η_{EQE}, PF contributed 10.3% and DF contributed 5.1%. The DF ratio was maintained at 33% (Fig. 3b) because the same parameter settings were used for the DPANIF emitter. As illustrated in Figs. 1 and 2, the PF emission produced in the DMPPP:DPANIF TTL contributed 10.3% of the record-high η_{EQE} value, and the DF emission produced in the NPAN:DPANIF TTF EML contributed 5.1% of the record-high η_{EQE} value. To confirm these efficiency results, two auxiliary OLEDs based on this high-efficiency device structure were fabricated by separately utilizing DMPPP:5% DPANIF and NPAN:3% DPANIF as a single EML (15 nm) in the devices. Coincidentally, the DMPPP- and NPAN-OLEDs exhibited an identical maximum η_{EQE} of 10.5% (Fig. 3a and **Table 3**; for detail EL characteristics, see **Supplementary Fig. S7**). By evaluating the TREL results, these two devices differed in the EL mechanism. The DMPPP-OLED exhibited no delayed emission, rendering it a fluorescent device with a great PF η_{EQE} of 10.5%, which dominated the PF contribution (η_{EQE} = 10.3%) of the high-efficiency Hyper-2 TTF-OLED. According to **equations (1)** and **(2)**, the theoretical η_{LE} value was nearly 0.42 in the DMPPP-OLED; this was derived under the assumptions that η_{Re} and χ were 1. Obviously, NPAN-OLED is a TTF-device that exhibited a DF emission with a ratio of

11% in TREL signal to divide the 10.5% η_{EQE} into PF η_{EQE} of 9.3% and DF η_{EQE} of 1.1%. From the PF η_{EQE} value, a theoretical η_{LE} value of 0.38 was deduced in the NPAN-OLED. The low DF η_{EQE} indicated that a severe TPQ effect decayed the triplet exciton usage because of the high amount of h^+ polarons filled the EML of the reference single-EML TTF device; this finding is similar previously reported results regarding high-efficiency blue TTF-OLEDs (Fig. 3c and **Supplementary Table S1**) [20,22,23,,,]. For example, Kido *et al.* reported a high maximum η_{EQE} value of 12% and a DF emission ratio of 15%[22]. Therefore, one can be noted that the Hyper-2 device not only retained the advantage of high PF η_{EQE} in the DMPPP TTL but also boosted the DF η_{EQE} in the NPAN TTF EML by 4.2-fold by inhibiting TPQ effects. The record-high η_{EQE} was attributed to the aforementioned hyper–TTF mechanism involving the separation of the carrier recombination and TTF zones and inhibition of h^+ entry into the TTF layer. Particularly, the PF and DF contribution in TTF-OLEDs can be individually adjusted to determine the device η_{EQE}, which allows for greater progress than traditional TTF-OLEDs. Future upgraded efficiency of the hyper–TTF-OLED is still possible by employing new TTF materials of higher efficiency and more sophisticated PLQY emitters.

Conclusion

In summary, we demonstrated a novel hyper–TTF mechanism and its blue OLED structure by introducing a TTL adjacent to the TTF EML to maximize the usage of singlet and triplet excitons. The hyper–TTF-EML structure can separate the carrier recombination zone (in the TTL) away from the TTF EML and inhibit the entry of hole carriers into the TTF EML to reduce hole-induced TPQ effects. The TPQ was a crucial mechanism for reducing the usage of triplet excitons in traditional single-EML TTF-OLEDs. Without consideration of the balance between exciton generation and hole-induced TPQ, the hyper TTF-OLED provides a straightforward approach to optimize the contribution from the prompt and delayed fluorescence by fine-tuning the TTL and TTF EML, respectively. Among well-known commercial blue TTF-OLEDs composed of anthracene- and pyrene-based materials, our hyper–TTF-OLED achieved a record-high η_{EQE} of 15.4% with a 33% triplet exciton usage at minimum. Of course, it is possible to raise the triplet usage to reach greater efficiency performance in the future.

Methods

OLEDs were fabricated by depositing organic and inorganic layer onto a patterned ITO glass, pre-cleaned by O_2 plasma treatment, utilizing a multisource thermal evaporator. Organic and inorganic layers were deposited under high vacuum of 1×10^{-6} and 8×10^{-6} torr, respectively. After layer deposition, the devices were transferred into an N_2 glovebox for encapsulation. Device performances were measured by a brightness-current-voltage (BIV) system comprising a spectrometer (Minolta CS-1000), a source meter (Keithley 2400) and a LabVIEW program. Time-resolved EL (TREL) setup was consisted of a function generator (Agilent 33500B), a source meter (Keithley 2400), a photomultiplier (PMT, Hamamatsu H6780-20) and an oscilloscope (Tektronix TDS2004C). To separate the contribution from blue and green emissions, a 450-nm short pass (Thorlabs FESH0450) and a 600-nm long pass (FEL0600) filters were

placed in the front of devices. PLQY measurement system was consisted of a white light source (Horiba, PowerArc), an integrating sphere (Quanta-φ manual Rev C F-3029), a monochromator (Horiba, iHR320), and a PMT. After excited the samples in integrating sphere, all light energy was collected into a monochromator through optical fiber and then detected by a PMT to analyze the η_{PLQY} value by a Horiba software (FluorEssence).

Declarations

Acknowledgements

This work was supported by the Ministry of Science and Technology (MOST), Taiwan, under Grants MOST 110-2222-E-002-003-MY3, 109-2622-E-155-014, 108-2221-E-155-051-MY3, 108-2912-I-155-504, 108-2811-E-155-504, 107-2221-E-155-058-MY3, 107-2221-E-002-156-MY3, the MEGA project, which has received funding from the European Union's Horizon 2020 research and innovation programme under the Marie Skłodowska-Curie grant agreement No 823720.

Author contributions

Dr. Chia-Hsun Chen, Mr. Pei-Hsi Lee, Ms. Hung-Yi Lin and Dr. Bo-Yen Lin performed the device fabrication and measurements. Dr. Shih-Wen Wen and Prof. Man-kit Leung gave the chemistry consulting. Prof. Tien-Lung Chiu and Prof. Jiun-Haw Lee instructed the device design and measurement, and handle the paper submission.

Competing interests

The authors declare no competing interests.

References

[1] Baldo, M. A., O'Brien, D. F., Thompson, M. E. & Forrest, S.R. Excitonic singlet-triplet ratio in a semiconducting organic thin film. Phys. Rev. B 60, 14422–14428 (1999).

[2] Lee, J. H. et al. Blue organic light-emitting diodes: current status, challenge, and future outlook. J. Mater. Chem. C 7, 5874–5888 (2019).

[3] Baldo, M. A. et al. Highly efficient phosphorescent emission from organic electroluminescent devices. Nature 395, 151–154 (1998).

[4] Baldo, M. A., Lamansky, S., Burrows, P. E., Thompson, M. E. & Forrest S. R. Very high-efficiency green organic light-emitting devices based on electrophosphorescence. Appl. Phys. Lett. 75, 4–6 (1999).

[5] Adachi, C., Baldo, M. A., Thompson, M. E. & Forrest, S. R. Nearly 100% internal phosphorescence efficiency in an organic light-emitting device. J. Appl. Phys. 90, 5048–5051 (2001).

[6] Cui, L.S., Nomura, H., Geng, Y., Kim, J. U., Nakanotani, H. & Adachi, C. Controlling singlet–triplet energy splitting for deep-blue thermally activated delayed fluorescence emitters. Angew. Chem. Int. Ed. 56, 1571–1575 (2017).

[7] Lin, T. C. et al. Probe exciplex structure of highly efficient thermally activated delayed fluorescence organic light emitting diodes. Nat. Commun. 9, 1–8 (2018).

[8] Uoyama, H., Goushi, K., Shizu, K., Nomura, H. & Adachi, C. Highly efficient organic light-emitting diodes from delayed fluorescence. Nature 492, 234–238 (2012).

[9] Zhang, Q. et al. Efficient blue organic light-emitting diodes employing thermally activated delayed fluorescence. Nat. Photonics 8, 326–332 (2014).

[10] Im, Y. et al. Molecular design strategy of organic thermally activated delayed fluorescence emitters. Chem. Mater. 29, 1946–1963 (2017).

[11] Andruleviciene, V. et al. TADF versus TTA emission mechanisms in acridan and carbazole-substituted dibenzo[a,c]phenazines: towards triplet harvesting emitters and hosts. Chem. Eng. J. 417, 127902 (2021).

[12] Song, D., Zhao, S., Luo, Y. & Aziz, H. Causes of efficiency roll-off in phosphorescent organic light emitting devices: triplet-triplet annihilation versus triplet-polaron quenching. Appl. Phys. Lett. 97, 268 (2010).

[13] Xiang, C. et al. Efficiency roll-off in blue emitting phosphorescent organic light emitting diodes with carbazole host materials. Adv. Funct. Mater. 26, 1463–1469 (2016).

[14] Chen, H. W. et al. Liquid crystal display and organic light-emitting diode display: present status and future perspectives. Light: Sci. Appl., 7, 17168 (2018).

[15] Jung, H. et al. High efficiency and long lifetime of a fluorescent blue-light emitter made of a pyrene core and optimized side groups. ACS Appl. Mater. Interfaces 10, 30022–30028 (2018).

[16] Gao, C. et al. Application of triplet–triplet annihilation upconversion in organic optoelectronic devices: advances and perspectives. Adv. Mater. 2100704 (2021) [DOI: doi.org/10.1002/adma.202100704]

[17] Im, Y. et al. Recent progress in high-efficiency blue-light-emitting materials for organic light-emitting diodes. Adv. Funct. Mater, 27 1603007 (2017).

[18] Yang, X., Xu, X. & Zhou, G. Recent advances of the emitters for high performance deep-blue organic light-emitting diodes. J. Mater. Chem. C 3, 913–944 (2015).

[19] Chen, Y. H. et al. Superior upconversion fluorescence dopants for highly efficient deep-blue electroluminescent devices. Chem Sci. 7, 4044–4051 (2016).

[20] Chou, P.Y. et al. Efficient delayed fluorescence via triplet-triplet annihilation for deep-blue electroluminescence. Chem. Commun. 50, 6869–6871 (2014).

[21] Wang, L. et al. New blue host materials based on anthracene-containing dibenzothiophene. Org. Electron. 12(4), 595–601 (2011).

[22] Hu, J. Y. et al. Bisanthracene-based donor–acceptor-type light-emitting dopants: highly efficient deep-blue emission in organic light-emitting devices. Adv. Funct. Mater. 24, 2064–2071 (2014).

[23] Wang, S. et al. Efficient deep-blue electrofluorescence with an external quantum efficiency beyond 10%. iScience 9, 532–541 (2018).

[24] Lim, H. et al. Enhanced triplet–triplet annihilation of blue fluorescent organic light-emitting diodes by generating excitons in trapped charge-free regions. ACS Appl. Mater. Interfaces 11, 48121–48127 (2019).

[25] Ieuji, R., Goushi, K. & Adachi, C. Triplet–triplet upconversion enhanced by spin–orbit coupling in organic light-emitting diodes. Nat. Commun. 10, 5283 (2019).

[26] Coehoorn, R., Bobbert, P. A. & van Eersel, H. Förster-type triplet-polaron quenching in disordered organic semiconductors. Phys. Rev. B 96(18), 184203 (2017).

[27] Coehoorn, R., Bobbert, P. A. & van Eersel, H. Effect of exciton diffusion on the triplet-triplet annihilation rate in organic semiconductor host-guest systems. Phys. Rev. B, 99, 024201 (2019).

[28] Chen, C. H. et al. Efficient triplet–triplet annihilation upconversion in an electroluminescence device with a fluorescent sensitizer and a triplet-diffusion singlet-blocking layer. Adv. Mater., 30, 1804850 (2018).

[29] Erickson, N. C. & Holmes, R.J. Engineering efficiency roll-off in organic light-emitting devices. Adv. Funct. Mater. 24, 6074–6080 (2014).

[30] Erickson, N. C. & Holmes, R. J. Investigating the role of emissive layer architecture on the exciton recombination zone in organic light-emitting devices. Adv. Funct. Mater. 23, 5190–5198 (2013).

[31] Chen, C. H. et al. Efficient solid-state triplet-triplet annihilation up-conversion electroluminescence device by incorporating intermolecular intersystem-crossing dark sensitizer. Chem. Eng. J. 427, 130889 (2022).

[32] Kondakov, D. Y. Triplet-triplet annihilation in highly efficient fluorescent organic light-emitting diodes: current state and future outlook. Philos. Trans. Royal Soc. A 373, 20140321 (2015).

[33] Fukagawa, H. et al. Anthracene derivatives as efficient emitting hosts for blue organic light-emitting diodes utilizing triplet–triplet annihilation. Org. Electron. 13, 1197–1203 (2012).

[34] Hu, L. et al. Efficient dendrimers based on naphthalene indenofluorene for two-photon fluorescent imaging in living cells and tissues. J. Mater. Chem. C 8, 2160–2170 (2020).

[35] Lüssem, B., Riede, M. & Leo, K. Doping of organic semiconductors. Phys. Status Solidi. 210, 9–43 (2013).

[36] Miyata, K., Conrad-Burton, F. S., Geyer, F. L. & Zhu, X. Y. Triplet pair states in singlet fission, Chem. Rev. 119, 4261–4292 (2019).

[37] Tang, X. et al. Efficient nondoped blue fluorescent organic light-emitting diodes (OLEDs) with a high external quantum efficiency of 9.4% @ 1000 cd m−2 based on phenanthroimidazole-anthracene derivative. Adv. Funct. Mater. 28, 1705813 (2018).

[38] Liu, W. et al. Nondoped blue fluorescent organic light-emitting diodes based on benzonitrile-anthracene derivative with 10.06% external quantum efficiency and low efficiency roll-off. J. Mater. Chem. C 7, 1014–1021 (2019).

[39]. Huh, J. S., Ha, Y. H., Kwon, S. K., Kim, Y. H. & Kim, J. J. Design strategy of anthracene-based fluorophores toward high-efficiency deep blue organic light-emitting diodes utilizing triplet–triplet fusion. ACS Appl. Mater. Interfaces 12, 15422–15429 (2020).

Tables

Table 1 | EL characteristics of reference TTF- and hyper–TTF-OLEDs at their maximum h_{EQE}.

Device	CIE*x,y*	Max. h_{EQE} (%)	DF ratio (%)	PF h_{EQE} (%)	DF h_{EQE} (%)
Reference	(0.15, 0.08)	2.59	7	2.41	0.18
Hyper	(0.15, 0.07)	5.41	47	2.88	2.53

Table 2 | EL characteristics of Alq_3-probe hyper–TTF-OLEDs. Derived h_{EQE} values of hyper–TTF-OLEDs with and without Alq_3 probe at current density of 2.5 mA·cm^{-2}, which was close to their maximum values. PF and DF ratios were analysed using TREL. Blue and green ratios were determined though spectral splitting. ([a]proportion)

Position	Max. h_{EQE} (%)	Blue PF h_{EQE} (%)	Blue DF h_{EQE} (%)	Green PF h_{EQE} (%)	Green DF h_{EQE} (%)
N.A.	5.41	2.88 (0.53)[a]	2.53 (0.47)[a]	-	-
−4.5 nm	4.65	1.75 (0.38)[a]	2.15 (0.46)[a]	0.75 (0.16)[a]	0
0.5 nm	4.19	2.23 (0.53)[a]	1.10 (0.26)[a]	0.37 (0.09)[a]	0.49 (0.12)[a]
9.5 nm	3.94	2.10 (0.53)[a]	1.17 (0.30)[a]	0.24 (0.06)[a]	0.43 (0.11)[a]

Table 3 | Electroluminescent characteristics of high-efficiency OLEDs at their maximum h_{EQE}.

Device	CIE*x,y*	h_{EQE}	DF ratio (%)	PF h_{EQE}	DF h_{EQE}
Hyper 1	(0.137, 0.153)	8.8%	33	5.9%	2.9%
Hyper 2	(0.134, 0.180)	15.4%	33	10.3%	5.1%
DMPPP	(0.137, 0.167)	10.5%	0	10.5%	0
NPAN	(0.135, 0.159)	10.5%	11	9.3%	1.2%

Figures

Figure 1

Energy transfer dynamics, molecular structures, device EL performances, and triplet-polaron quenching. a, Schematic of traditional and hyper–TTF mechanisms. **b,** Schematic of energy level and energy transfer dynamics in DMPPP/ADN EML of hyper–TTF-OLED and the corresponding molecular structures. **c,** TREL signals of reference and hyper–TTF-OLEDs after a driving current density of 4 mA·cm^{-2}. **d,** h_{EQE}, PF h_{EQE} (light colour bar), and DF h_{EQE} (dark colour bar) values observed at various current densities for reference TTF- and hyper–TTF-OLEDs. **e,** I_{TTF} of TTF EOD and HOD under various current densities normalized by $I_{TTF,0}$ (no current); I_{TTF} represents DF PL intensity at 450 nm (ADN emission) under an excitation of 532 nm (PtOEP absorption).

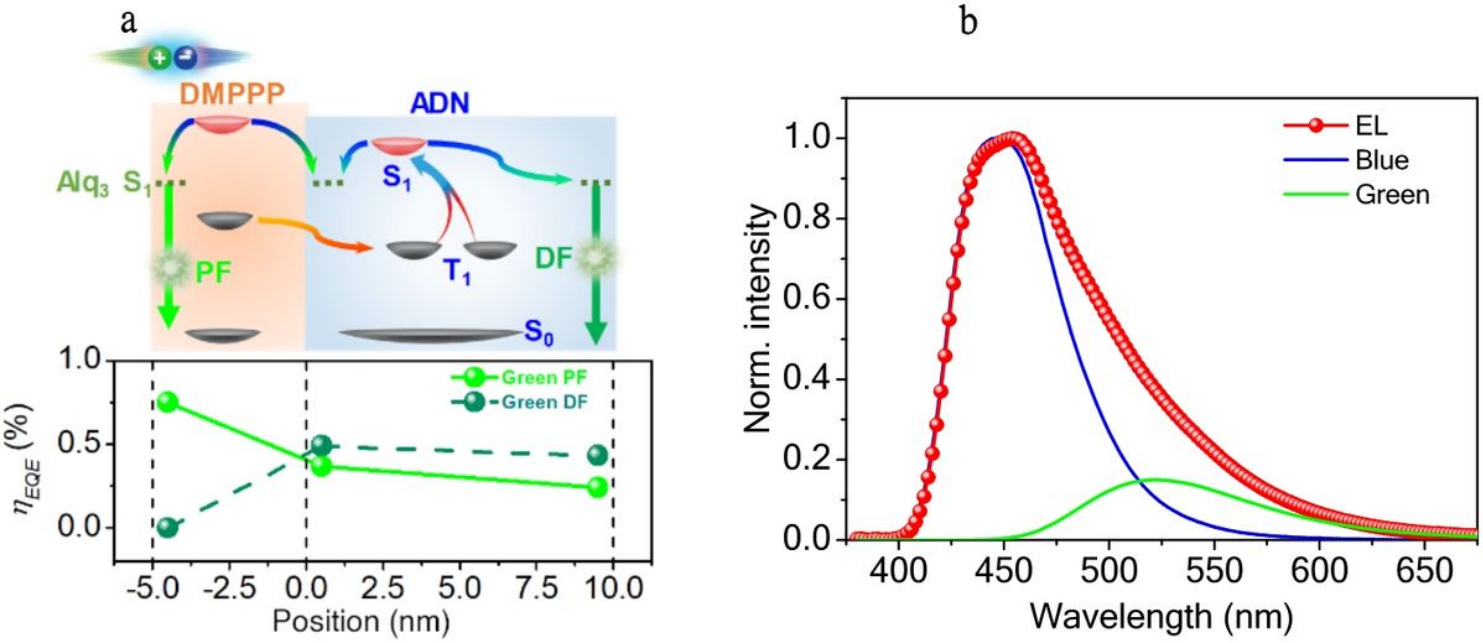

Figure 2

Energy transfer diagram and electroluminescent performances of selectively dopant devices. a, Energy transfer diagram of Alq_3 probers (···dotted line) in hyper–TTF-OLEDs (upper graph); Alq_3 was selectively doped at −4.5, 0.5 and 9.5 nm away from the DMPPP/ADN interface. The green PF and DF h_{EQE} (lower graph) are analyzed according to the TREL behaviors. **b,** Spectral splitting achieved by dividing normalised EL spectrum (at 2.5 mA·cm^{-2}) into blue (ADN) and green (Alq_3) spectra to determine their contribution proportion.

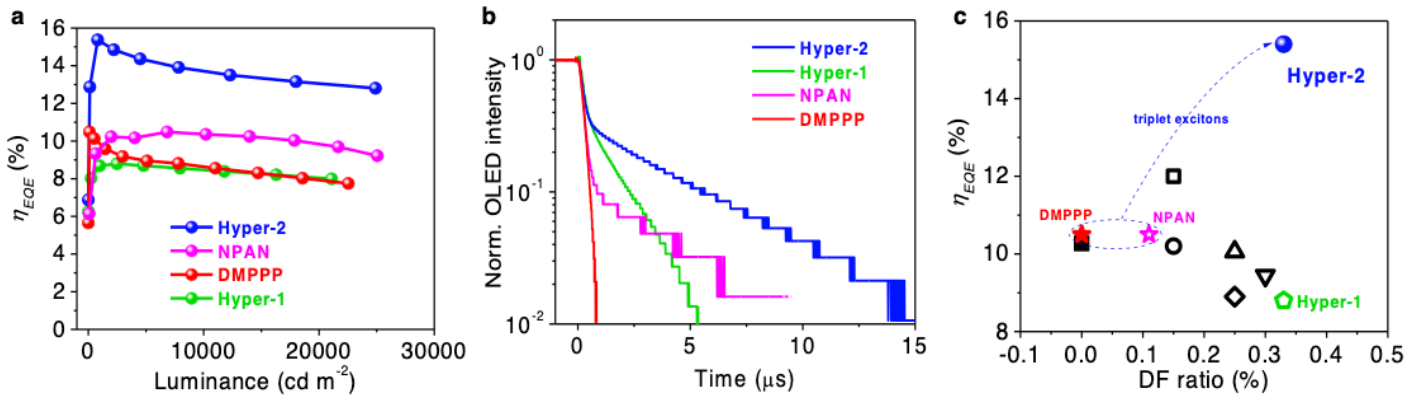

Figure 3

Electroluminescent performances of high-efficiency OLEDs. Four blue OLEDs consisting of two hyper–TTF-OLEDs (Hyper 1 and 2), one fluorescent OLED (DMPPP), and one TTF-OLED (NPAN). **a,** h_{EQE} versus luminance. **b**, TREL signals after a driving current density of 4 mA·cm^{-2}. **c**, h_{EQE} versus DF ratio ranking with the reported values (ref. 20 ●; ref. 22 □; ref. 23 ■; ref. 37 Ñ; ref. 38 Δ; ref. 39 ◊)

Supplementary Files

This is a list of supplementary files associated with this preprint. Click to download.

- 202101019HyperTTFpaperSIv2.docx
- Onlinefloatimage1.png